



Article

Spatially Modeling the Synergistic Impacts of Global Warming and Sea-Level Rise on Coral Reefs in the South China Sea

Xiuling Zuo ^{1,2,†}, Fenzhen Su ^{3,†}, Kefu Yu ^{1,2,4,*} , Yinghui Wang ^{1,2}, Qi Wang ⁵ and Huisheng Wu ⁶

¹ Guangxi Laboratory on the Study of Coral Reefs in the South China Sea, Guangxi University, Nanning 530004, China; zuoxl@gxu.edu.cn (X.Z.); wyh@gxu.edu.cn (Y.W.)

² School of Marine Sciences, Guangxi University, Nanning 530004, China

³ State Key Laboratory of Resources and Environmental Information System, Institute of Geographic Sciences and Natural Resources Research, CAS, Beijing 100101, China; sufz@lreis.ac.cn

⁴ Southern Marine Science and Engineering Guangdong Laboratory (Zhuhai), Zhuhai 519080, China

⁵ School of Surveying and Geo-Informatics, Shandong Jianzhu University, Jinan 250101, China; wangqi19@sdjzu.edu.cn

⁶ College of Oceanography and Space Informatics, China University of Petroleum (Huadong), Qingdao 266580, China; wuhuisheng@upc.edu.cn

* Correspondence: kefuyu@scsio.ac.cn

† Shared first authorship.

Abstract: Global warming and sea-level rise (SLR) induced by rising atmospheric CO₂ concentrations can cause coral bleaching, death, and submergence of the world's coral reefs. Adopting the GIS and RS methods, we modeled how these two stressors combine to influence the future growth of the atolls and table reefs of three archipelagoes in the South China Sea (SCS), based on geomorphic and ecological zones. A large-scale survey of the coral communities in Xisha Islands in 2014, Dongsha Islands in 2014–2016 and Nansha Islands in 2007 provided zone-specific process datasets on the range of reef accretion rates. Sea surface temperature and extreme (minimum and maximum) SLR data above 1985–2005 levels by 2100 in the SCS were derived from the Intergovernmental Panel on Climate Change (IPCC) Fifth Assessment Report (AR5) models forced with the Representative Concentration Pathways (RCPs). Our model projected that: (1) the Xisha Islands and Dongsha Islands may have a better growth status, because the reef flat biotic sparse zone may be recolonized with hard coral and become a biotic dense zone; (2) the southern Nansha Islands reefs have a risk of stopping growing due to their earlier annual bleaching years. The increasing of water depths of these reefs is stronger in the RCP with more emissions. Our approach offers insights into the best-case and worst-case impacts of two global environmental pressures on potential future reef growth under a changing climate.

Keywords: global warming; sea-level rise; coral reefs; spatial model; south China sea



Citation: Zuo, X.; Su, F.; Yu, K.; Wang, Y.; Wang, Q.; Wu, H. Spatially Modeling the Synergistic Impacts of Global Warming and Sea-Level Rise on Coral Reefs in the South China Sea. *Remote Sens.* **2021**, *13*, 2626. <https://doi.org/10.3390/rs13132626>

Academic Editor: John Burns

Received: 19 May 2021

Accepted: 30 June 2021

Published: 4 July 2021

Publisher's Note: MDPI stays neutral with regard to jurisdictional claims in published maps and institutional affiliations.



Copyright: © 2021 by the authors. Licensee MDPI, Basel, Switzerland. This article is an open access article distributed under the terms and conditions of the Creative Commons Attribution (CC BY) license (<https://creativecommons.org/licenses/by/4.0/>).

1. Introduction

Since the industrial revolution began at the start of the 19th century, the burning of fossil fuels and the unprecedented increases in the amount of atmospheric carbon dioxide (CO₂) and other greenhouse gas have caused a marked increase in the temperatures of the atmosphere and ocean, and widespread ice sheets to melt and sea-level to rise [1]. Anthropogenic global warming has created a serious threat to coral reef ecosystems around the world with widespread coral bleaching events being related to the increase of sea surface temperatures (SSTs) [2–4]. Coral bleaching can drive major reductions in reef carbonate production as well as reef growth potential [4–6], and often leads to mortality when temperature stress persists [7]. The third worldwide coral bleaching event since 1990 happened in 2014–2017, killed corals and reef organisms over thousands of square kilometers [3]. The future of global coral reef ecosystems under global warming has been predicted using coupled ocean–atmosphere general circulation models (GCMs) [2,8–10]. These projections show that widespread coral bleaching event will become more frequent

on most global coral reefs by the mid-21st century or earlier. Some reefs experiencing later bleaching may provide temporary refuge for reef species [2].

Observations suggest that climate change is causing global sea-level to rise, and the tropical Pacific Ocean flourished with lots of global low-lying atolls has the highest sea-level rise (SLR) rate [11]. Sea-level is projected to rise about 26–82 cm by 2081–2100 compared with 1986–2005 [1]. SLR affects coral reefs by altering their environment, including local hydrodynamics and duration of emergence at low tide. Coral reef flats in many Indo-Pacific reefs are colonized by few corals due to their exposure at low tide. A higher sea level may provide space for corals to recolonize, including horizontal extension and vertical growth [12,13], resulting in a more productive reef community. Conversely, SLR will increase wave energy passing over reefs to shore, increasing the risk to reef islands and infrastructures [11,14–16]. Rapidly increasing sea-level could also result in ‘drowned’ reefs, for instance in Hawaii [17], as the reef is submerged past depth limits supporting coral growth [18]. Therefore, SLR may play the role of stressor or opportunity, relying on its rise rate and the ability of the reef to keep pace.

Projections show that coral bleaching events induced by climate change have driven major declines in reef accretion potential, resulting in the increase rates of reef submergence under future SLR [19,20]. However, how future coral bleaching and SLR from global warming will combine to influence the growth of coral reefs is largely unknown. Topography is an essential control on reef growth that is constructed by generations of reef scleractinian corals and associated organisms accreting over geological timescales of decades to millennia [21]. The carbonate production rates are the highest on reef slopes and decline on reef flats dominated by algae, mollusks, and benthic foraminifera dominate [12,22–24]. Projections of the response of coral reefs to global warming and SLR, using carbonate data from different topographic areas of the reef, may help to better understand the capacity of reefs to track future climate change.

Over two hundred coral reefs are located in the South China Sea (SCS). The SCS is the largest marginal sea in southeastern Asia. These reefs are experiencing global warming and SLR like other tropical reefs [25,26]. The average SST in summer in the SCS suggests an uptrend of 0.2 °C per decade. However, the spatial pattern has a high heterogeneity, with a marked uptrend in the region of the northern and western SCS [26]. The ecological carrying capacity of the coral reefs in the Xisha Islands in these waters decreased by nearly 60% from 2007 to 2015, and the increase in ocean temperatures caused by global warming indirectly caused its ecological degradation [27,28]. However, local SLR was 16.2 ± 0.6 cm from 1987 to 2016 in the northern SCS, and the inshore Sanya Bay reef flat, where sustained coral growth is widely considered as marginal, was recolonized by corals [29].

Here, we used data collected from the geomorphic and ecological zones mapped by satellite images of 12 reefs among the atolls and table reefs of three archipelagoes across the SCS to explore the geospatial responses of the archipelagoes to combined global warming and SLR under the Intergovernmental Panel on Climate Change (IPCC) Fifth Assessment Report (AR5) Representative Concentration Pathways (RCPs) scenarios by 2100 in Geographical Information System (GIS) software. We compared our calculated reef accretion rate in different geomorphic and ecological zones against annual bleaching as well as extreme (minimum and maximum) SLR rates projected under the RCP2.6, RCP4.5, and RCP8.5 scenarios. Our aims were to: (1) study the response variations in the same geomorphic or ecological zone among different reefs across three archipelagoes and the response variations between different zones in the same reef; (2) predict the capacity of the reef zone to track future predicted rates of SLR and global warming, and project total minimum and maximum water depth increases in each zone by 2100.

2. Materials and Methods

2.1. Study Area

The study area was the atolls and table reefs of the Xisha Islands, Dongsha Islands, and Nansha Islands in the SCS. The SCS covers about 3.5 million km² and locates in about

3°N–24°N. It contains over 200 reefs which can be separated into four archipelagoes. The Dongsha Islands are the northernmost archipelago in the SCS, with the smallest number of reefs, and one atoll, Dongsha atoll. Together 101 coral species have been recorded there [30]. The Xisha Islands comprise ~36 reefs, most of which are atolls and table reefs. There are a total of 37–38 genera and 127 species and subspecies of scleractinian corals recorded [31]. The large Nansha Islands include more than 230 atolls, table reefs, submerged reefs, and shoals. There are more than 50 genera and 200 species of scleractinian corals, which is about one-third of the Indo-Pacific scleractinian coral species. The Nansha Islands is the most biologically diverse marine region in the SCS [32].

In the study area, the summer monsoon prevails from late May to mid-September, and the winter monsoon prevails from late October to early in the following April. The monthly mean SST is 22°–29 °C in the northern Dongsha Islands, 24°–29 °C in the Xisha Islands, and 26.8°–30.3 °C in the Nansha Islands located in the southern SCS [26].

Coral growth data in this study came from 12 reefs in the three archipelagoes (Figure 1), with 9 reefs from the Xisha Islands, 1 reef from the Dongsha Islands [33,34], and 2 reefs from the Nansha Islands [35]. Data for the Dongsha Islands and Nansha Islands were derived from previous literatures.

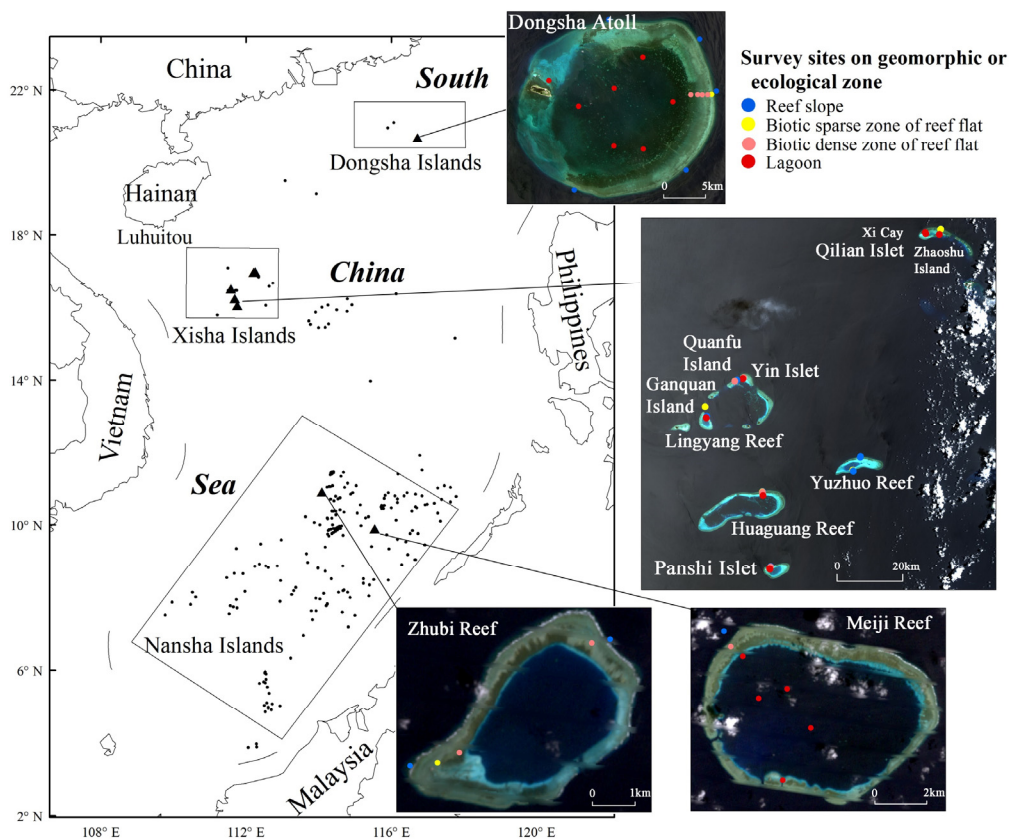


Figure 1. Location of field data sites in the Xisha Islands, South China Sea: Xi Cay and Zhaoshu Island of Qilian Islet, Yin Islet, Quanfu Island, Ganquan Island, Lingyang Reef, Huaguang Reef, Panshi Islet, Yuzhuo Reef; Dongsha Islands: Dongsha Atoll (derived from Decarlo et al., 2017 [34]; Tkachenko and Soong, 2017 [33]); Nansha Islands: Zhubi Reef and Meiji Reef (derived from Zhao et al., 2013 [35]). Blue dots represent the sites at the reef slope, gold dots represent the sites at the biotic sparse zone of the reef flat, pink dots represent the sites at the biotic dense zone of the reef flat, red dots represent the sites in the lagoon. The sites are overlaid on the Gaofen-1 moderate spatial resolution image (16 m × 16 m pixel size) acquired on 30 May 2014 in Xisha Islands and on 8 May 2015 in Dongsha atoll, as well on the Landsat ETM+ multi-spectral and pan fusion moderate spatial resolution images (15 m × 15 m pixel size) acquired on 17 February 2007 in Meiji Reef and on 8 February 2007 in Zhubi Reef.

2.2. Field Survey and Data Extraction

The latest research indicates that there is great zonal difference within atolls and table reefs in the SCS, and the common zones are reef slopes, reef crests, the biotic sparse zones of the reef flat, the biotic dense zones of the reef flat, and lagoons [36–38]. Field benthic community videos at 54 sites in different geomorphic and ecological zones on eight atolls and table reefs of Xisha Islands were recorded from 1 to 7 June 2014. The inventory of geomorphic and ecological zones was guided by satellite imagery from Landsat ETM+ and mapped using the satellite image in the ArcGIS 10.2 software. Those zones were distinguished based on color and texture differences presented on the satellite images [36], just as we supposed that color and texture differences indicated diverse habitats. Ground verification of geomorphic and ecological zones was realized by following 20 m transects across the reef where the substrate has visual changes on the remote sensing image. Videos of the substrates were taken at a height from 0.5 m to 1.5 m by a snorkeler or diver, depending on the water clarity. The beginning and finish positions of each transect were recorded using a hand-held GPS with an accuracy of 1 m on a small boat.

The benthic cover and composition of transects were analyzed in the lab by CPCe software and 10 coordinate points were randomly selected on each JPEG, converted from digital videos [39]. Community structure was classified into the following eight categories: live hard coral, dead coral, bleached coral, coral skeletal fragments, sand, rock, seagrass, and macroalgae. Live hard coral in the transect was identified to genus and species levels and morphological level (such as, *Acropora* branching or *Porites* massive) following the work of Veron (2000) [40]. To be consistent with the field investigation, the final geomorphic or ecological zones of survey reefs were mapped using the same method based on a Gaofen-1 (GF-1) 16 m multispectral satellite image of the Xisha Islands captured on 30 May 2014. The field points were loaded on the geomorphic and ecological map in ArcGIS 10.2 to examine the accuracy of the map and derive the zones they showed. The accuracy of the map was evaluated using a confusion matrix and the metrics included the overall accuracy, the user accuracy, and the producer accuracy [41]. The overall accuracy is calculated by dividing the total correctly classified sample sites (i.e., the sum of the major diagonal sample sites) by the number of total sample sites in the confusion matrix.

Coral communities (including genus, species and morphology) in Dongsha atoll in the Dongsha Islands as well as Zhubi Reef and Meiji Reef in the Nansha Islands were derived from published literatures. The Dongsha atoll was surveyed on the reef flat in the end of May and the beginning of June 2014 [34], and on the reef slope and lagoon in August–September 2016 [33]. Zhubi Reef and Meiji Reef were surveyed in May and June 2007 [35]. Following testing and verification at the Xisha Islands, we applied the resulting mapping method for the Xisha Islands to a GF-1 satellite image of the Dongsha Islands derived on 8 May 2015, as well as a Landsat ETM+ 15 m multi-spectral and pan fusion images of the Nansha Islands captured on 17 February 2007 (Meiji Reef) and on 8 February 2007 (Zhubi Reef) to map the geomorphic and ecological zones of these reefs and derive the zone locations of the survey sites. As data are missed at the narrow reef crest, and the accretion within the lagoon is dependent on sediment production by organisms such as foraminifera and *Halimeda* algae and the importation of sediment from other areas [42,43], the study of reef responses to global warming and SLR are based on the reef slope, biotic sparse zone of reef flat, and biotic dense zone of reef flat.

2.3. Modelling Reef Response to Global Warming and Sea-Level Rise Scenarios from 2014 to 2100

2.3.1. Climate Model and Thermal Stress Calculation

The IPCC AR5 advanced the development of the Coupled Model Intercomparison Project (CMIP5), which uses RCPs. Many GCMs are included in the CMIP5, which are provided with higher spatial resolution and are more complex than before [44]. However, large uncertainties still exist in the simulation of historical and future SST in these GCMs [45]. Here, the earth system model of the Canadian Centre for Climate Modelling and Analysis (CanESM2) was selected for simulation as it can better reproduce the primary character-

istics and variations of the historical SST in the SCS. Moreover, the linear trends of SST derived from CanESM2 of RCP4.5 and RCP8.5 scenarios in the next century (2006–2099) in the SCS agree well with the multimodel ensemble average trend and they are only slightly higher in the RCP2.6 scenario than those from the multimodel ensemble [46].

Monthly variable “tos” (Sea Surface Temperature) for the RCP2.6, RCP4.5, and RCP8.5 scenarios were retrieved from the CanESM2 model from the World Climate Research Programme’s CMIP5 dataset3 (<http://cmip-pcmdi.llnl.gov/cmip5/> (accessed on 13 May 2014)) using ArcGIS 10.2 software. To make the start data of CanESM2 be consistent with the satellite observed SST climatology, the average SST of CanESM2 were corrected employing observed data from the NOAA Optimal Interpolated SST(OISST) V2 (<http://www.esrl.noaa.gov/psd/> (accessed on 5 July 2014)) [47]. Model deviation at each location was eliminated by subtracting the average data in 2006–2011 of CanESM2. The average OISST climatology from 1982 to 2005 was then added to the whole dataset [48].

In 1982–2005 climatological data, the maximum monthly mean (MMM) was calculated according to the warmest month at each location. Degree heating weeks (DHWs) began to accumulate when SSTs were greater than the MMM [2]. Degree heating months (DHMs) are derived using the sum of above positive anomalies within three months and was then transformed to DHWs by multiplying by 4.34. For each grid-cell ($1^\circ \times 1^\circ$), we projected the year after which 10 bleaching events (>6 DHWs) per decade are expected [2], which is regarded as a metric for the unsustainability year for coral reefs. Projections were shown only for reef locations in the SCS. A map of the annual bleaching scenario (10 per decade) was produced using the ArcGIS 10.2 software for each RCP experiment.

2.3.2. Sea-Level Rise Scenarios

Temperature and thermal expansion projections from 21 CMIP5 models by the IPCC AR5 indicated that the global mean SLR will reach about 26–55 cm at the end of this century (2081–2100) in the RCP2.6 scenario, 32–63 cm in the RCP4.5 scenario, and 45–82 cm in the RCP8.5 scenario, relative to that in 1986–2005 [49]. The SLR predictions are also variable spatially among ocean basins due to the influence of wind and ocean circulation [50,51]. The spatial pattern is well presented for SST, but local SLRs are expected to be fairly constant, even at the scale of the SCS basin [52,53]. The multimodel ensemble mean dynamic SLR projected in the SCS is only -0.2 – 2.1 cm, 0.6 – 2.6 cm, and -0.3 – 2.5 cm during the same period according to 24 CMIP5 models by the IPCC AR5, resulting in a total SLR of 25.8–57.1 cm, 32.6–65.6 cm, and 44.7–84.5 cm in the RCP2.6, RCP4.5, and RCP8.5 scenarios, respectively [25]. This outcome is identical with sea level obtained from reconstruction data over past decades, which indicates that the sea level fluctuations in the SCS follow with the global mean SLR from long-term trend [54]. The projections of extreme (minimum and maximum) SLR in three scenarios in SCS were selected in simulation. These were a minimum SLR of 25.8 cm (2.72 mm year $^{-1}$), 32.6 cm (3.43 mm year $^{-1}$), 44.7 cm (4.7 mm year $^{-1}$), and a maximum SLR of 57.1 cm (6.01 mm year $^{-1}$), 65.6 cm (6.91 mm year $^{-1}$), 84.5 cm (8.89 mm year $^{-1}$) in RCP2.6, RCP4.5, and RCP8.5, respectively.

2.3.3. Parameterization of Reef Accretion

The coral genera, genera coverage, and calcification rate of each genera were integrated to calculate the coral carbonate production rates [55]. The calcification rate for coral genera in the SCS was adopted [22]. For the missing calcification rate for some genera, we chose that of other coral genera of the same family or similar growth forms. The average coral carbonate production rate for each geomorphic or ecological zone was represented by the mean \pm standard deviation. The coralline algae production was calculated based on published average rates of crustose coralline algae (CCA) calcification in the Indo-Pacific [56]. The gross carbonate production was computed as the total of calculated carbonate production by scleractinian corals and coralline algae. The mean 25% of community calcification was estimated to convert into upward reef accretion, and the remaining portion was considered as bioerosion or mechanical disruption and transporta-

tion to other environments of the reef system [22,57]. Then, potential accretion rates for the reef slope, biotic sparse zone of reef flat and biotic dense zone of reef flat was calculated using carbonate density and framework porosity [20,58].

2.3.4. Simulation Model Construction and Implementation

To evaluate the capacity of the coral reefs in our study area to follow projected sea level changes, and to assess variations of water depth by 2100, we compared our calculated reef accretion data combined with the appearance of annual bleaching against local sea-level change data. The simulation model was constructed based on four factors: the initial time of reef growth, the water depth of the zone where the reef grows, reef accretion rate, and the relationship between reef growth and sea-level variation Equation (1). These reflected the critical properties of gross reef morphological change over time [59]. This model was implemented from 2014 to 2100. For each grid-cell, the upward reef accretion G_a , was computed for the given timestep according to the upward annual reef accretion rate G'_a and annual bleaching year, and added to the existing status of the geomorphic or ecological zone of the reef platform Equation (2). The SLR across an equivalent time step was subtracted from the upward reef accretion to build a new model showing the vertical position of the coral reef platform relative to the sea surface in 2100 Equation (1).

$$\Delta H = Z_{2100} - Z_{2014} = SLR - G_a \quad (1)$$

where

Z_{2100} : water depth of geomorphic or ecological grid-cell in 2100 (cm).

Z_{2014} : water depth of geomorphic or ecological grid-cell in 2014 (cm).

G_a : upward reef accretion of geomorphic or ecological grid-cell during time 2014 to 2100 (cm).

SLR : sea-level rise during time interval from 2014 to 2100 (cm).

$$G_a = (Y_{annual} - 2014) \times G'_a \times 0.1 \quad (2)$$

Y_{annual} : annual bleaching year of geomorphic or ecological grid-cell (reef slope, biotic sparse zone of reef flat and biotic dense zone of reef flat) in RCPs.

G'_a : upward annual reef accretion rate for geomorphic or ecological grid-cell (mm year^{-1}).

3. Results

3.1. Sites of Geomorphic or Ecological Zones in Simulation

The geomorphic and reef flat ecological map of the surveyed reefs in three archipelagoes is shown in Figure 2. The Xisha Islands mapping assessment is shown in Table 1. The geomorphic and reef flat ecological zones were mapped with 94.4% overall accuracy using our mapping method (Table 1). Errors of omission were highest for the biotic sparse zone of reef flat (producer's accuracy = 77.8%) and the biotic dense zone of reef flat (user's accuracy = 81.8%) (Table 1). Based on the mapping method, the number of field sites in each geomorphic or ecological zone in the three islands was calculated (Table 2).

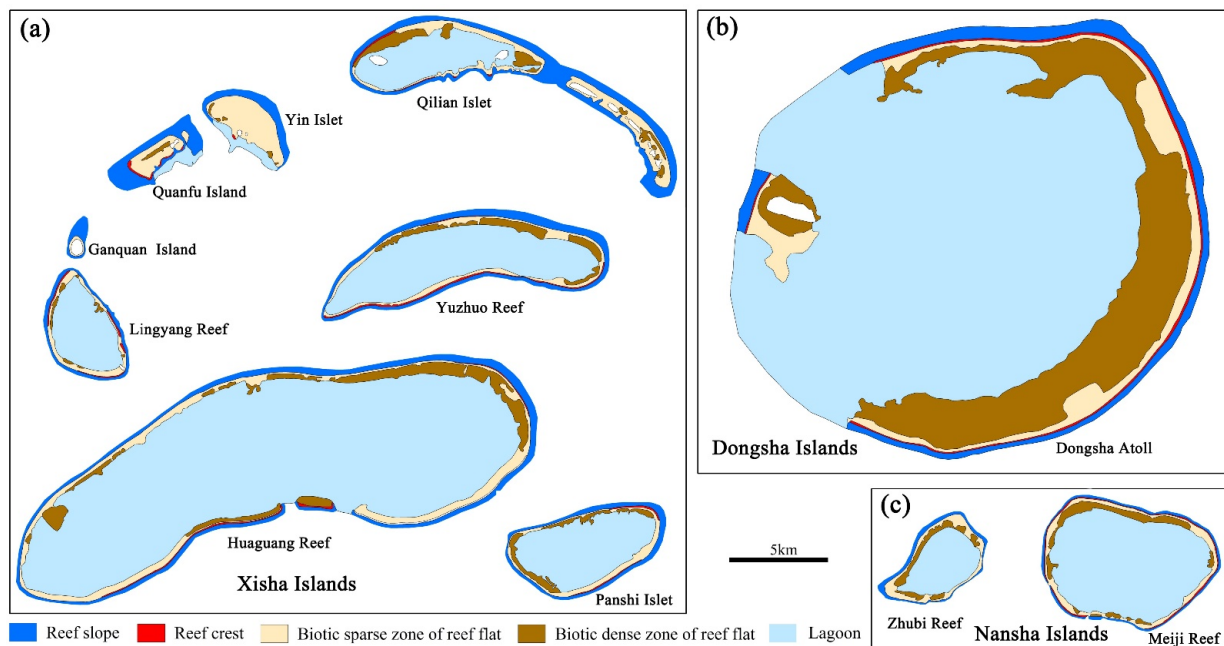


Figure 2. The geomorphic and reef flat ecological map of the surveyed reefs in (a) Xisha Islands, (b) Dongsha Islands, and (c) Nansha Islands.

Table 1. Confusion matrix for geomorphic and reef flat ecological mapping in the Xisha Islands. Overall accuracy = 94.4%.

	Remote Sensing Interpretation					User's Accuracy
	Reef Slope	Biotic Sparse Zone of Reef Flat	Biotic Dense Zone of Reef Flat	Lagoon	Total Sites	
Reef slope	16	0	0	0	16	100%
Biotic sparse zone of reef flat	0	7	1	0	8	87.5%
Biotic dense zone of reef flat	0	2	9	0	11	81.8%
Lagoon	0	0	0	19	19	100%
Total sites	16	9	10	19	54	-
Producer's accuracy	100%	77.8%	90%	100%	-	-

Table 2. Number of field sites used for modeling in geomorphic and reef flat ecological zones for the Xisha Islands, Dongsha Islands, and Nansha Islands.

Reef/Geomorphic	Xisha Islands	Dongsha Islands	Nansha Islands
Reef slope	16	10	3
Biotic sparse zone of reef flat	8	1	2
Biotic dense zone of reef flat	11	6	5
Total	35	17	10

3.2. Accretion Rate of Geomorphic or Ecological Zones

Based on field survey data, the net carbonate production rates of reef framework ranged from 0.72 to 10.13 kg m⁻² year⁻¹ (Table 3). The highest rates were computed at sites on the reef slope (range 5.22–10.13 kg m⁻² year⁻¹) (Table 3); while lowest rates were on the biotic sparse zone of reef flat (range 0.72–2.63 kg m⁻² year⁻¹). We note that carbonate production is mainly driven by the similar coral genera on most reef slopes.

The relative abundance of *Acropora*, *Montipora*, *Pocillopora* and *Porites* differed among the sites in the three islands, but they together contributed on average >70% of the produced coral carbonate. Carbonate production on the biotic dense zone of reef flat is predominantly driven by *Montipora* in the Xisha Islands and Nansha Islands, and by *Stylophora* in the Dongsha Islands. The largest difference in coral communities between the three islands

appeared on the reef flat biotic sparse zone. However, because hard coral cover in the biotic sparse zone is very low, the difference in coral communities has the least influence on the coral carbonate production.

Table 3. Summary of characteristics of survey sites and of reef biological communities derived carbonate production and reef accretion rate (± 1 sd) calculated for 9 reefs in the Xisha Islands ($n = 35$, 20 m transects); 1 reef in Dongsha Islands ($n = 17$, 50 m transects on the reef flat and 25 m transects on the reef slope); and 2 reefs in Nansha Islands ($n = 10$, 20 m transects).

	Reef Slope			Biotic Sparse Zone of Reef Flat			Biotic Dense Zone of Reef Flat		
	Xisha	Dongsha	Nansha	Xisha	Dongsha	Nansha	Xisha	Dongsha	Nansha
Live coral cover	30.34 \pm 14.86	51.36 \pm 12.16	21.11 \pm 25.76	7.62 \pm 7.75	6.0 \pm 0.0	4.24 \pm 0.2	44.36 \pm 24.06	24.83 \pm 5.56	31.84 \pm 19.16
Coral production (kg/m ² /year)	10.11 \pm 5.44	12.09 \pm 3.39	5.99 \pm 7.36	1.35 \pm 1.71	1.92 \pm 0.00	0.9 \pm 0.05	9.26 \pm 1.58	7.43 \pm 2.17	6.9 \pm 4.43
Dominant coral genus and % contribution to total coral carbonate production	<i>Montipora</i> (74.2%)	<i>Acropora</i> (41.7%)	<i>Montipora</i> (50.4%)	<i>Acropora</i> (50.5%)	<i>Stylophora</i> (87.9%)	<i>Psammocora</i> (42.4%)	<i>Montipora</i> (90.5%)	<i>Stylophora</i> (63.4%)	<i>Montipora</i> (62.4%)
	<i>Pocillopora</i> (6.8%)	<i>Montipora</i> (25.5%)	<i>Acropora</i> (21.7%)	<i>Montipora</i> (29.9%)	<i>Acropora</i> (10.6%)	<i>Porites</i> (15.2%)		<i>Acropora</i> (22.9%)	<i>Heliopora</i> (20.3%)
	<i>Acropora</i> (5.8%)	<i>Pocillopora</i> (9.3%)	<i>Porites</i> (13.2%)			<i>Pocillopora</i> (12.7%)		<i>Porites</i> (13.0%)	
			<i>Pocillopora</i> (9.0%)						
Coralline algal production (kg/m ² /year)	1.57 \pm 2.14	1.41 \pm 0.52	0.98 \pm 0.66	0.36 \pm 0.78	1.59 \pm 0.00	0.06 \pm 0.03	3.32 \pm 2.63	0.09 \pm 0.17	0.96 \pm 0.62
Gross biological carbonate production (kg/m ² /year)	11.68 \pm 6.10	13.50 \pm 3.91	6.97 \pm 6.87	1.71 \pm 1.63	3.51 \pm 0.00	0.96 \pm 0.02	12.58 \pm 4.57	7.52 \pm 2.15	7.87 \pm 4.34
Net biological carbonate production (kg/m ² /year)	8.76 \pm 4.57	10.13 \pm 2.93	5.22 \pm 5.15	1.28 \pm 1.22	2.63 \pm 0.00	0.72 \pm 0.01	9.44 \pm 3.43	5.64 \pm 1.61	5.91 \pm 3.25
Reef accretion rates (mm year ⁻¹)	6.06 \pm 2.81	7.01 \pm 2.03	3.62 \pm 3.57	0.89 \pm 0.85	1.82 \pm 0.00	0.50 \pm 0.01	4.67 \pm 1.70	3.90 \pm 1.12	4.09 \pm 2.25

Low-carbonate production rates are reflected in low reef accretion rates calculated on the biotic sparse zone of reef flat across the SCS. In the Xisha Islands and Nansha Islands, the mean reef accretion rate was 0.89 mm year⁻¹ and 0.5 mm year⁻¹, respectively, while it was 1.82 mm year⁻¹ in the same zone of the Dongsha Islands. The highest reef accretion rates were calculated at the reef slope of the Dongsha Islands (7.01 \pm 2.03 mm year⁻¹). They were lower in the Xisha Islands (6.06 \pm 2.81 mm year⁻¹) and the Nansha Islands (3.62 \pm 3.57 mm year⁻¹). Similar reef accretion rates of about 4 mm year⁻¹ characterized all biotic dense zones of reef flat examined in the SCS (Xisha Islands, 4.67 \pm 1.70 mm year⁻¹; Dongsha Islands, 3.90 \pm 1.12 mm year⁻¹; Nansha Islands, 4.09 \pm 2.25 mm year⁻¹; Table 3).

3.3. Reef Responses to Global Warming

The annual bleaching year for archipelagoes in the SCS (Figure 3) was calculated from the SST in the different RCPs of CanESM2. The median year when coral bleaching events begin to happen every year on global reef sites is 2046 for RCP 2.6, 2047 for RCP 4.5, and 2040 for RCP 8.5, projected by combinations of IPCC AR5 models [2]. Reefs in the southeastern part of the Nansha Islands were predicted 5–15 years earlier to experience annual bleaching than the global median year (orange color, Figure 3), under the RCP4.5 and RCP8.5 scenarios. Higher latitude reefs will experience annual bleaching conditions later. Annual bleaching events occurred on reefs five years or more than the global median year (blue color and green color, Figure 3) included the Xisha Islands, Dongsha Islands, and the northern and western parts of the Nansha Islands. These reefs can be regarded as temporary refuges for corals in the SCS. The spatial patterns of annual bleaching were very similar among three scenarios (Figure 3), but different reef locations experienced annual bleaching conditions earlier especially in the RCP8.5 scenario.

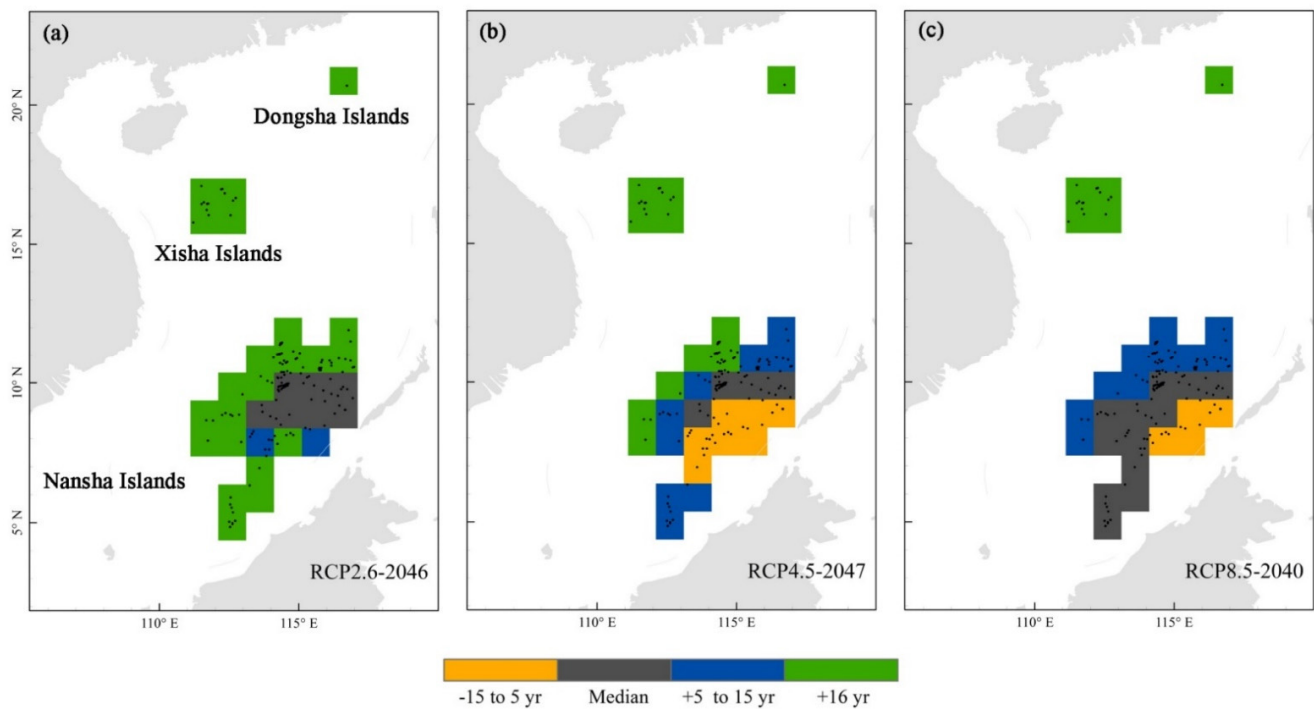


Figure 3. Maps for (a) Representative Concentration Pathway (RCP) 2.6, (b) RCP4.5, and (c) RCP8.5 showing years that reef locations of the South China Sea (SCS) begin to experience annual bleaching conditions (color scale). Global median values (a) 2046, (b) 2047 and (c) 2040 calculated by Van Hooidonk et al. (2013) [2] are shown next to the RCP labels and are represented by gray color.

3.4. Reef Responses to Global Warming and Sea-Level Rise

The reef accretion rate in geomorphic or ecological zones in 2014 and the extreme (minimum and maximum) SLR rate in the RCP scenarios in the SCS are shown in Figure 4. The minimum SLR rate in RCP2.6 was higher than the reef accretion rate in the biotic sparse zone of reef flat. The maximum SLR rate in RCP2.6 was only lower than the reef accretion rate on the reef slope of the Xisha Islands and Dongsha Islands. The maximum SLR rate in RCP 8.5 was higher than the reef accretion rate of all the zones.

Atolls and table reefs responded differently to the synergistic global warming and SLR scenarios (Figure 5). Shallow reef slopes will catch up with SLR first due to the higher reef accretion rate and then water depths may increase if there are annual bleaching conditions. The decrease of the water depth of reef slopes is about 0–40 cm by 2100 when there are no annual bleaching conditions before 2100 under the minimum SLR of RCP2.6. These reefs are the Xisha Islands and Dongsha Islands in the minimum SLR of RCP2.6 and RCP4.5 scenarios (Figure 5a,b). In the minimum SLR of RCP8.5, no reef will experience a decrease of water depth by 2100 (Figure 5c). Shallow reef slopes that experience annual bleaching earlier sink more clearly and this signal is more obvious in the maximum SLR scenarios (Figure 5j–l) than in the minimum SLR scenarios (Figure 5a–c). In the maximum SLR of RCP8.5, water level of the reef slopes in the southeastern part of the Nansha Islands may increase about 60–80 cm (Figure 5l).

During the entire tidal cycle, the increased water depth over the biotic sparse zone of reef flat will result in this area being underwater. Therefore, the vertical constraints which previously restricted coral growth will be progressively eliminated and this zone will be recolonized with hard coral across the eighty-year period simulated. With the minimum SLR in RCP2.6, the zone platform is likely to progress slowly through an initial stage of coral colonization on shallow surfaces for the first 55–80 years [12]; for the first 40–60 years with the minimum SLR in RCP4.5; and for the first 30–40 years with the minimum SLR in RCP8.5. With the maximum SLR, coral recolonization progresses more rapidly and needs 20–30 years in RCP2.6, 15–25 years in RCP4.5, and 10–20 years in RCP8.5, respectively. The

current reef accretion rate on the biotic dense zone of reef flat was used in modeling when biotic sparse zone was recolonized with hard coral. Reef flat biotic sparse zones without annual bleaching conditions will change into the biotic dense zones, and then catch up with SLR by 2100. These reefs include the Dongsha Islands, Xisha Islands, and the northern and western parts of Nansha Islands in minimum SLR of RCP2.6 and RCP4.5 scenarios (Figure 5d,e). Biotic sparse zones that experience annual bleaching conditions earlier than the coral recolonization year may not experience coral recolonization and water depths will increase by 2100. These reefs include the southeastern part of the Nansha Islands in the minimum SLR of three RCP scenarios (Figure 5d–f). Other reefs in this zone with later annual bleaching conditions (Figure 5d–f,m–o) will be recolonized with hard coral first and then water depths may increase. The water level of biotic sparse zones in the Nansha Islands will increase about 0–60 cm in the minimum SLR of RCPs (Figure 5d–f), and about 20–100 cm in the maximum SLR of RCPs (Figure 5m–o).

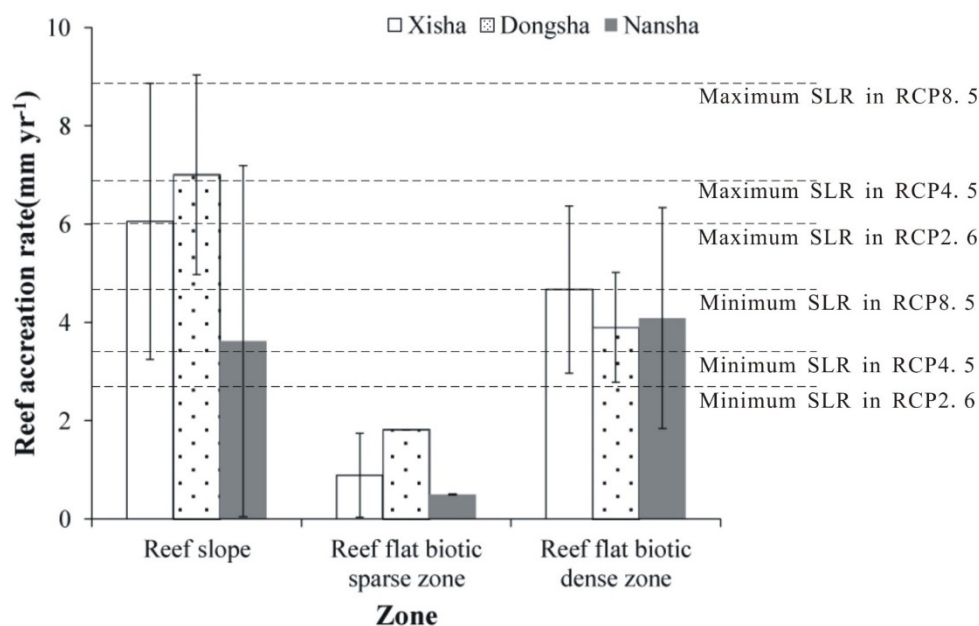


Figure 4. Reef accretion rate in geomorphic or ecological zones in the Xisha Islands, Dongsha Islands and Nansha Islands and the extreme (minimum and maximum) sea-level rise (SLR) under RCP2.6, RCP4.5, and RCP8.5 in the South China Sea (SCS).

Most biotic dense zones without annual bleaching conditions by 2100 may keep up with SLR by adjusting the reef accretion rate following the change in vertical space influenced by SLR. These different responses to changes in accommodation space have been recorded in the fossil, including examples of ‘keep up’ type of reef growth and limited aggradation because of the reduced accommodation space [60]. These reefs include the Dongsha Islands, Xisha Islands, and the northern and western parts of the Nansha Islands in the minimum and maximum SLR of RCP2.6 and 4.5 scenarios (Figure 5g–h,p–q). Biotic dense zones experiencing annual bleaching conditions may experience water depths increasing and water level of this zone is deeper when there are larger CO₂ emissions and faster SLR rates, such as the maximum increase of the water depths (60–80 cm) in the Nansha Islands in the maximum SLR of RCP8.5 (Figure 5r).

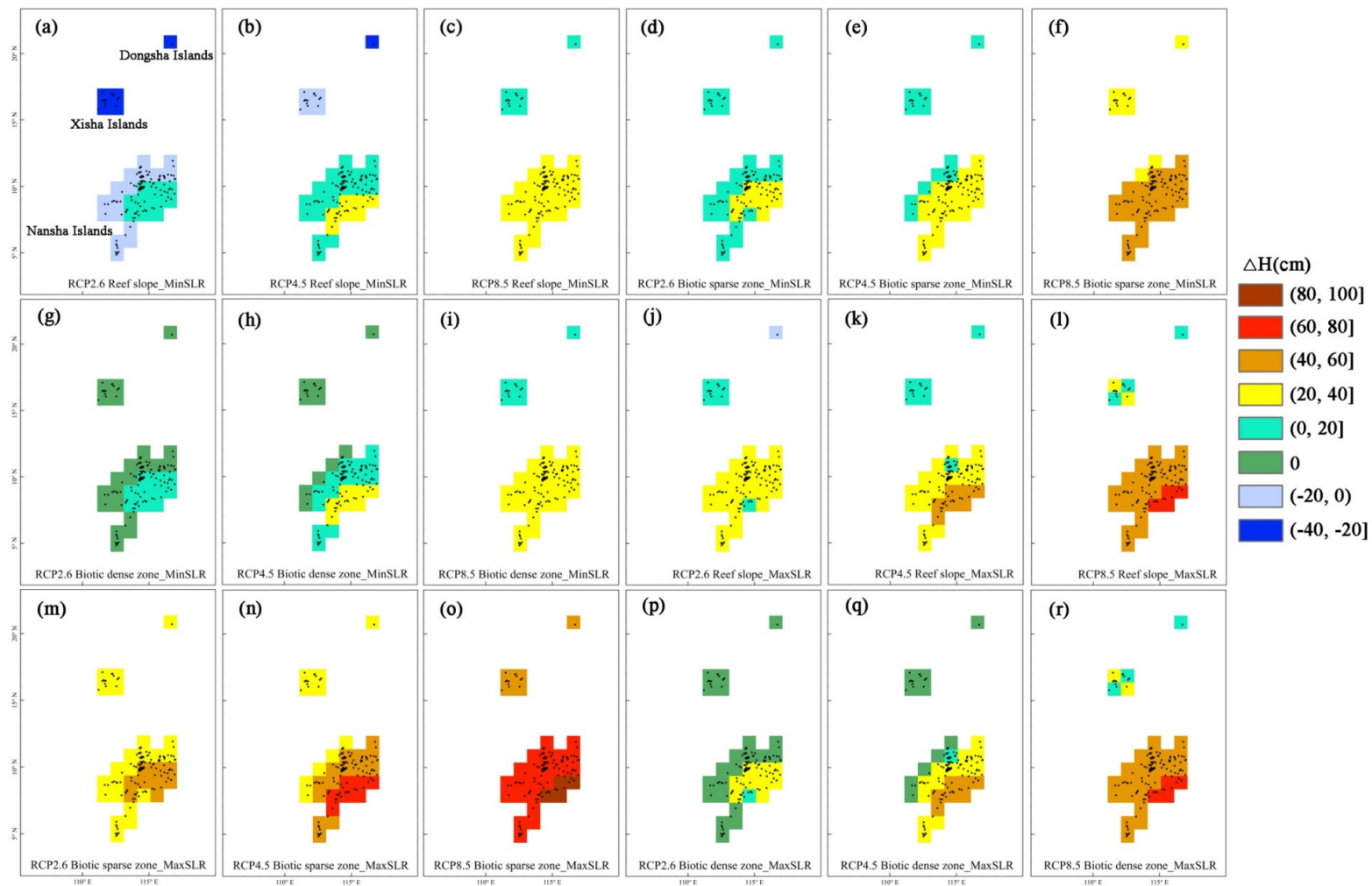


Figure 5. Projected bathymetry changes in geomorphic and reef flat ecological zones for atolls and table reefs above 2014 levels by 2100 in the South China Sea under global warming and minimum sea-level rise (minSLR) and maximum sea-level rise (maxSLR) under RCP2.6, RCP4.5 and RCP8.5. (a–c,j–l) are for reef slopes; (d–f,m–o) are for biotic sparse zones of reef flat; (g–i,p–r) are for biotic dense zones of reef flat.

4. Discussions

4.1. Computed Parameters Versus Published Data

Our high coral carbonate production rates from the *Acropora*-dominated reef slope (average $10.13 \pm 2.93 \text{ kg m}^{-2} \text{ year}^{-1}$, Dongsha Islands, Table 3) are near the production rates (range ~ 5 to $9 \text{ kg m}^{-2} \text{ year}^{-1}$) reported as typical of Indo-Pacific reef slope environments dominated by *Acropora* [24]. The coral carbonate production of the biotic dense zone of reef flat (Dongsha Islands, $5.64 \pm 1.61 \text{ kg m}^{-2} \text{ year}^{-1}$; Nansha Islands, $5.91 \pm 3.25 \text{ kg m}^{-2} \text{ year}^{-1}$) is also close to the outer reef-flats production (around $4 \text{ kg m}^{-2} \text{ year}^{-1}$) in the Pacific [23].

The reef accretion rates among the three Island groups make little difference. The reef accretion rate calculated on the shallow reef slope in the three Island groups is comparable with $2.1\text{--}8.8 \text{ mm year}^{-1}$ for the reef slope in central Java, Indonesia [61]. The reef accretion rate of $0.89 \text{ mm year}^{-1}$ and 0.5 mm year^{-1} on the biotic sparse zone of reef flat of Xisha Islands and Nansha Islands is similar to the $0.6 \pm 0.3 \text{ mm year}^{-1}$ on the reef flat of Luhuitou fringing reef in the SCS [22], and to $0.86 \text{ mm year}^{-1}$ on the reef flat of Warraber Island in Australia [57]. Although the biotic dense zone of reef flat accretes faster than the biotic sparse zone due to the dense live coral cover, similar reef accretion rates of about 4 mm year^{-1} characterize all biotic dense zones. Therefore, our rates fit within a common range, indicating reef accretion potential estimated are reasonable for different zones in the SCS.

4.2. Isolating the Impacts of Global Warming and Sea-Level Rise

Projections of annual bleaching conditions in SCS based on the CanESM2 model of IPCC AR5 showed a latitudinal gradient with reefs at higher latitudes experiencing annual bleaching conditions later. This pattern is much stronger in RCP4.5 and RCP8.5 than in RCP2.6 (Figure 3). The southeastern part of the Nansha Islands experienced annual bleaching conditions earlier than the global median year (Figure 3) in most RCPs and may be the most seriously affected region. This is consistent with the higher warming rate ($0.2^\circ\text{--}0.4^\circ \text{C/decade}$) calculated from the mean satellite SST in summer from 1982 to 2009 in this area [26]. Coral bleaching events from field surveys or fossil records have also been reported in Nansha Islands [62]. The Dongsha Islands also have had a higher warming rate in recent decades (about $0.3^\circ\text{--}0.4^\circ \text{C/decade}$) [26], but they will be the last to experience annual bleaching conditions in the projection (Figure 3). We note that the time interval through which annual bleaching conditions were evaluated differed nearly four-fold with the period from 1982–2009. While recent warming trends may exactly replicate historical trends over a long period of time, they might be also affected by ocean fluctuations (e.g., Pacific Decadal Oscillation), which can enhance or weaken the short-term trend.

The responses of reefs that do not experience annual bleaching conditions over this century show the importance of SLR. These reefs include the Dongsha Islands, Xisha Islands, and the northern and western parts of Nansha Islands in RCP2.6 and RCP4.5 scenarios (Figure 3). SLR has the greatest impact on the biotic sparse zone of reef flat (Figure 4). The biotic sparse zone of reef flat in SCS is similar to many reef flats of Indo-Pacific, which are colonized by few corals as the exposure at the low tide restricted their growth [63]. Water depths increases from sea-level rise may expand space for corals to colonize, finally leading to horizontal and vertical growth, enabling further growth of corals on this zone. Evidence from coral reefs in the Pacific in clear waters, e.g., Heron Island, Australia [13], Palau [64], and Solomon Islands [63], suggests that sea-level rise can drive coral growth on the reef flats. Therefore, SLR may 'turn on' coral colonization where it has been 'turned off' before because of the limited accommodation space, and the maximum anticipated SLR of about 84.5 cm may be beneficial for many biotic sparse zones of reef flat. Moreover, this zone can be recolonized with hard coral earlier when SLR is faster.

SLR has minor effects on reef slopes (Figure 4). The accretion rate of the shallow reef slope of the three islands was higher than the minimum SLR rate in the RCP2.6 and RCP4.5 scenarios (Figure 4). These shallow reef slopes without annual bleaching conditions, may

first catch up and then keep up with SLR in these two scenarios. Many Indo-Pacific reefs after 6000 year BP caught up with sea level from water depths of 10–20 m [65]. However, when the accretion rates of shallow reef slopes are lower than the SLR rate (Figure 4), these zones would have a slight deepening of the habitats by 2100, such as Xisha Islands under the maximum SLR of RCP4.5 and RCP8.5 scenarios. Deeper benthic reef components after SLR may have no further accretion and can no longer compete. The biotic dense zone of reef flat may keep up with SLR. In the projections, corals may switch significantly from vertical extension seawards to lateral extension when the accretion rate is higher than the minimum SLR rate of RCP2.6 and 4.5 scenarios, and then from lateral growth to vertical growth when the accretion rate is lower than the maximum SLR of three RCP scenarios.

Over the past 30 years, local SLR of the northern SCS was 16.2 ± 0.6 cm [29], which is comparable with the trend of global mean sea level rise. Compared with the sea level rise rate of RCPs, the SLR rate in the northern SCS (5.4 mm year^{-1}) is close to the minimum SLR rate of RCP8.5. At this rate, reef slopes of the Xisha Islands and Dongsha Islands without annual bleaching conditions, may have the potentiality to closely catch up with SLR at the end of this century, while reef slopes of Nansha Islands may fall behind. The inshore coral reefs of the Sanya Bay flat in the northern SCS in highly degraded environments have already recolonized with hard coral due to recent SLR [29].

4.3. Synergistic Impacts of Global Warming and Sea-Level Rise

Annual bleaching conditions are not sustainable for corals. Reef zones that experience annual bleaching conditions get progressively deeper both in the minimum and maximum SLR of RCP2.6, RCP4.5, and RCP8.5 scenarios, and this will particularly affect areas such as the southeastern part of Nansha Islands, due to their earlier annual bleaching conditions (Figure 5). Biotic sparse zones in the southeastern part of the Nansha Islands in the minimum SLR of three RCP scenarios (Figure 5d–f) may not have enough time to be recolonized with coral and become inundated immediately as they experience annual bleaching conditions earlier. Other reefs of this zone with later annual bleaching conditions may be initially recolonized with hard coral and then water depths will increase after these corals die (Figure 5d–f,m–o). Reefs in the biotic dense zone of reef flat may keep up with SLR first and then water depths will increase when there are annual bleaching conditions (Figure 5g–i,p–r). Shallow reef slopes in the three islands with annual bleaching conditions will catch up with SLR first and then water depths will increase even with the minimum SLR of RCP2.6 and 4.5 (Figure 5a,b). The reefs that will keep up with SLR first and then water depths will increase are located in the Xisha Islands in maximum SLR of RCP2.6 and in the Dongsha Islands in maximum SLR of RCP4.5 (Figure 4). Reefs exhibit a tendency of water depths increasing during the whole period when SLR rate is higher than the reef accretion rate (Figure 4). Studies show that coral bleaching mortality usually diminishes with increasing water depth [66]. The 1998 catastrophic bleaching event caused ~90% coral mortality down to about 15 m depth in northern atolls in the Hawaiian Archipelago [67]. Deep water may be the coral refuges, where hard corals may continue growing.

Sediments of reef crest in Yongxing Island in Xisha Islands in the SCS consist of coral skeletal fragments, broken branches [68], and the reef crest is exposed at low tide. This zone may have a similar response to the biotic sparse zone of reef flat and be recolonized with hard coral over this century when the limitation of exposure at low tide disappears. Water depths of the reef crest may also increase after experiencing annual bleaching conditions with the continuing SLR. Exposed patch reefs in the lagoon in the SCS have clear but narrow zones (slope, crest, patchy flats). Some parts of the patchy flat have coral distribution similar to the reef flat biotic dense zone, while some parts have low hard coral cover [36]. Zones of patch reefs may have the same response as reef slope, reef crest, biotic sparse zone of reef flat or biotic dense zone of reef flat to global warming and SLR scenarios. Sheltered patch reefs in the lagoon 100% covered by *Porites* can keep up with SLR by switching from vertical extension seawards to lateral extension or lateral extension to vertical extension

when there are no annual bleaching conditions, but water depths may increase when there are annual bleaching conditions.

Compared with the projections of reefs, taking global warming or SLR into account individually, the water depths increasing of the reef slope and reef flat ecological zones shows the importance of synergistic consideration of global warming and SLR. It has been indicated that widespread shoreline erosion and inundation have appeared in response to recent global SLR [69]. Deepening water induced by global warming and SLR may increase wave erosion of the shoreline in future [70]. Atoll islands and table reefs will become increasingly unstable and experience potential human depopulation by the end of this century [11].

The past historical geological record on the influences of global warming and SLR on coral reefs in the SCS also shows this. In the middle Holocene in the SCS, sea levels were about 2–3 m higher than the present level and appeared in 7.0–5.5 ka BP. Then sea level fluctuated and decreased to the present level, matching the pattern of SST fluctuations [71] and demonstrating the close relationship between global warming and SLR. The shoreline retreated by 210 m due to the decrease of sea levels [72]. Repeated episodes of bleaching in the past 200 years have occurred on coral reefs in the southern portion of the SCS because of the high SST. Coral recovery after other environmental stress events in the mid-Holocene took an average about 10–20 years [73]. At present, corals in the SCS decline seriously which has significantly influenced their role and ecological function in the carbon cycle, such as the 80%–90% decrease of the CaCO_3 production of the Luhuitou fringing reef since 1960 due to the serious coral decline [22]. Protecting locations with oceanographic environment that result in lower thermal stress is important, such as the Dongsha Islands and Xisha Islands at relative higher latitudes (Figure 3). Our projections reflect the relative synergistic impacts of disturbances on coral reefs and can be viewed as an examination of the impact of the best-case and worst-case scenarios of global warming and SLR on coral reefs without consideration of other stressors.

4.4. Data Limitations

Due to this modeling effort's simplifying assumption, the possible mechanisms that will modify the prediction include the corals with remarkable physiological tolerances [74], coral adaptation to higher temperature [75,76], different communities more robust to waves [77,78], faster growing coral communities [79,80], and coral species in the deeper regions subjected to reduced light intensity and less severe storm events [81], etc. A time dependent variable G_a' in the model could adjust these "ecological factors" regularly.

The value of 0 for the reef accretion rate was adopted in simulations when annual bleaching occurred on coral reefs. In fact, resultant coral bleaching could also have either net positive carbonate budgets (4.2 mm year^{-1}) or net negative carbonate budgets ($-0.4 \text{ mm year}^{-1}$) [82]. If net negative carbonate budgets were expected to occur after experiencing annual bleaching conditions, the water level increase may have a stronger effect than at present.

5. Conclusions

We identified geomorphic and ecological zones to study the response of atolls and table reefs in three archipelagoes in the SCS to global warming and SLR from the datasets of IPCC climate change scenarios over this century based on GIS and RS methods. Simulations from 2014 to 2100 indicated that different geomorphic or ecological zones responded differently to global warming and SLR scenarios: the biotic sparse zone of reef flat without annual bleaching conditions may be recolonized with hard coral and turn into the biotic dense zone, including in the Dongsha Islands, Xisha Islands, and the northern and western parts of Nansha Islands in RCP2.6 and 4.5 scenarios. The reef slopes of the three archipelagoes will catch up with SLR initially and then water depths may increase about 0–40 cm in the Xisha Islands and Nansha Islands in the minimum SLR scenarios of RCP2.6 and RCP4.5. The geomorphic or ecological zones of reefs experiencing annual bleaching conditions

exhibited various degrees of water depths increasing (0–100 cm) and the water depths increasing of the Nansha Islands reefs were the most obvious in RCP8.5 due to their earlier annual bleaching years. Our study provided the best-case and worst-case scenarios of global warming and SLR on coral reefs without consideration of other stressors.

Author Contributions: Conceptualization, K.Y. and F.S.; methodology, X.Z. and F.S.; software, X.Z., Q.W. and H.W.; validation, X.Z., Q.W. and H.W.; formal analysis, X.Z.; investigation, X.Z., K.Y., F.S. and Y.W.; resources, F.S. and K.Y.; data curation, K.Y. and F.S.; writing—original draft preparation, X.Z.; writing—review and editing, X.Z.; visualization, X.Z.; supervision, K.Y. and F.S.; project administration, X.Z., K.Y. and F.S.; funding acquisition, X.Z., K.Y. and F.S. All authors have read and agreed to the published version of the manuscript.

Funding: This research was funded by the “National Natural Science Foundation of China, grant number 41801341, 42090041 and 42030502”, “Guangxi Natural Science Foundation of China, grant number 2018JJB150030”, “Guangxi scientific projects, grant number AD17129063 and AA17204074”, “BaGui Scholars Program Foundation, grant number 2014BGXZGX03”, “Innovation Project of Guangxi Graduate Education, grant number YCBZ2020006”, and “Strategic Priority Research Program of the Chinese Academy of Science, grant number XDA13010400”.

Data Availability Statement: Monthly output sea surface temperature data were retrieved from the CanESM2 model from the World Climate Research Programme’s CMIP5 dataset3 for the RCP2.6, RCP4.5, and RCP8.5 scenarios (<http://cmip-pcmdi.llnl.gov/cmip5/> (accessed on 13 May 2014)).

Acknowledgments: The authors would like to thank Wei Shi, Junmin Li and Guoliang Zhou for their important assistance in the field survey.

Conflicts of Interest: The authors declare no conflict of interest.

References

1. Stocker, T.F.; Qin, D.; Plattner, G.K.; Alexander, L.V.; Allen, S.K.; Bindoff, N.L.; Bréon, F.M.; Church, J.A.; Cubasch, U.; Emori, S. IPCC, 2013: Technical Summary. In *Climate Change 2013: The Physical Science Basis*; Intergovernmental Panel on Climate Change, Ed.; Cambridge University: New York, NY, USA, 2013; pp. 533–535.
2. Van Hooidonk, R.; Maynard, J.A.; Planes, S. Temporary refugia for coral reefs in a warming world. *Nat. Clim. Chang.* **2013**, *3*, 508–511. [[CrossRef](#)]
3. Hughes, T.P.; Kerry, J.T.; Alvarez-Noriega, M.; Alvarez-Romero, J.G.; Anderson, K.D.; Baird, A.H.; Babcock, R.C.; Bejer, M.; Bellwood, D.R.; Berkemans, R. Global warming and recurrent mass bleaching of corals. *Nature* **2017**, *543*, 373. [[CrossRef](#)] [[PubMed](#)]
4. Sheppard, C.; Sheppard, A.; Mogg, A.; Bayley, D.; Dempsey, A.; Roche, R.; Turner, J.; Purkis, S. Coral bleaching and mortality in the Chagos Archipelago. *Atoll Res. Bull.* **2017**, *613*, 1–26. [[CrossRef](#)]
5. Yan, H.; Shi, Q.; Yu, K.; Tao, S.; Yang, H.; Liu, Y.; Zhang, H.; Zhao, M. Regional coral growth responses to seawater warming in the South China Sea. *Sci. Total Environ.* **2019**, *670*, 595–605. [[CrossRef](#)]
6. Perry, C.T.; Morgan, K.M. Post-bleaching coral community change on southern Maldivian reefs: Is there potential for rapid recovery? *Coral Reefs* **2017**, *36*, 1189–1194. [[CrossRef](#)]
7. Hooidonk, R.V.; Huber, M. Quantifying the quality of coral bleaching predictions. *Coral Reefs* **2009**, *28*, 579–587. [[CrossRef](#)]
8. Logan, C.A.; Dunne, J.P.; Eakin, C.M.; Donner, S.D. Incorporating adaptive responses into future projections of coral bleaching. *Glob. Chang. Biol.* **2014**, *20*, 125–139. [[CrossRef](#)] [[PubMed](#)]
9. Meissner, K.J.; Lippmann, T.; Gupta, A.S. Large-scale stress factors affecting coral reefs: Open ocean sea surface temperature and surface seawater aragonite saturation over the next 400 years. *Coral Reefs* **2012**, *31*, 309–319. [[CrossRef](#)]
10. Van Hooidonk, R.; Maynard, J.; Tamelander, J.; Gove, J.; Ahmadi, G.; Raymundo, L.; Williams, G.; Heron, S.F.; Planes, S. Local-scale projections of coral reef futures and implications of the Paris Agreement. *Sci. Rep.* **2016**, *6*, 39666. [[CrossRef](#)]
11. Storlazzi, C.D.; Elias, E.P.L.; Berkowitz, P. Many atolls may be uninhabitable within decades due to climate change. *Sci. Rep.* **2015**, *5*, 14546. [[CrossRef](#)] [[PubMed](#)]
12. Hamylton, S.M.; Leon, J.X.; Saunders, M.I.; Woodroffe, C.D. Simulating reef response to sea-level rise at Lizard Island: A geospatial approach. *Geomorphology* **2014**, *222*, 151–161. [[CrossRef](#)]
13. Scopélitis, J.; Andréfouët, S.; Phinn, S.; Done, T.; Chabanet, P. Coral colonisation of a shallow reef flat in response to rising sea level: Quantification from 35 years of remote sensing data at Heron Island, Australia. *Coral Reefs* **2011**, *30*, 951–965. [[CrossRef](#)]
14. Sheppard, C.; Dixon, D.J.; Gourlay, M.; Sheppard, A.; Payet, R. Coral mortality increases wave energy reaching shores protected by reef flats: Examples from the Seychelles. *Estuar. Coast. Shelf Sci.* **2005**, *64*, 223–234. [[CrossRef](#)]
15. Storlazzi, C.D.; Elias, E.; Field, M.E.; Presto, M.K. Numerical modeling of the impact of sea-level rise on fringing coral reef hydrodynamics and sediment transport. *Coral Reefs* **2011**, *30*, 83–96. [[CrossRef](#)]

16. Kench, P.S.; Ford, M.R.; Owen, S.D. Patterns of island change and persistence offer alternate adaptation pathways for atoll nations. *Nat. Commun.* **2018**, *9*, 605. [[CrossRef](#)] [[PubMed](#)]
17. Webster, J.M.; Clague, D.A.; Riker-Coleman, K.; Gallup, C.; Braga, J.C.; Potts, D.; Moore, J.G.; Winterer, E.L.; Paull, C.K. Drowning of the –150 m reef off Hawaii: A casualty of global meltwater pulse 1A? *Geology* **2004**, *32*, 249–252. [[CrossRef](#)]
18. Woodroffe, C.D.; Webster, J.M. Coral reefs and sea-level change. *Mar. Geol.* **2014**, *352*, 248–267. [[CrossRef](#)]
19. Perry, C.T.; Murphy, G.N.; Graham, N.A.J.; Wilson, S.K.; Januchowskiahartley, F.A.; East, H.K. Remote coral reefs can sustain high growth potential and may match future sea-level trends. *Sci. Rep.* **2015**, *5*, 18289. [[CrossRef](#)] [[PubMed](#)]
20. Perry, C.T.; Alvarezfilip, L.; Graham, N.A.J.; Mumby, P.J.; Wilson, S.K.; Kench, P.S.; Manzello, D.P.; Morgan, K.M.; Slangen, A.B.A.; Thomson, D.P. Loss of coral reef growth capacity to track future increases in sea level. *Nature* **2018**, *558*, 396–400. [[CrossRef](#)] [[PubMed](#)]
21. Done, T. Corals: Environmental controls on growth. In *Encyclopedia of Earth Sciences*; Hopley, D., Ed.; Springer: Dordrecht, The Netherlands, 2011; pp. 281–293.
22. Shi, Q.; Zhao, M.; Zhang, Q.; Yu, K.; Chen, T.; Li, S.; Wang, H. Estimate of carbonate production by scleractinian corals at Luhuitou fringing reef, Sanya, China. *Chin. Sci. Bull.* **2009**, *54*, 696–705. [[CrossRef](#)]
23. Smith, S.V.; Kinsey, D.W. Calcium carbonate production, coral reef growth, and sea level change. *Science* **1976**, *194*, 937–939. [[CrossRef](#)] [[PubMed](#)]
24. Vecsei, A. A new estimate of global reefal carbonate production including the fore-reefs. *Glob. Planet. Chang.* **2004**, *43*, 1–18. [[CrossRef](#)]
25. Huang, C.; Qiao, F. Sea level rise projection in the South China Sea from CMIP5 models. *Acta Oceanol. Sin.* **2015**, *34*, 31–41. [[CrossRef](#)]
26. Zuo, X.; Su, F.; Wu, W.; Chen, Z.; Shi, W. Spatial and temporal variability of thermal stress to China's coral reefs in South China Sea. *Chin. Geogr. Sci.* **2015**, *25*, 159–173. [[CrossRef](#)]
27. Wu, Z.; Wang, D.; Tu, Z. The analysis on the reason of hermatypic coral degradation in Xisha. *Acta Oceanol. Sin.* **2011**, *33*, 140–146.
28. Zhang, Z.; Shao, K.; Yang, Z. Evaluation of the Xisha coral reef ecosystem carrying capacity. *Mar. Environ. Sci.* **2018**, *37*, 487–492. (In Chinese)
29. Chen, T.; Roff, G.; McCook, L.; Zhao, J.; Li, S. Recolonization of marginal coral reef flats in response to recent sea-level rise. *J. Geophys. Res. Oceans* **2018**, *123*, 7618–7628. [[CrossRef](#)]
30. Dai, C.F.; Fan, T.Y.; Wu, C.S. Coral fauna of Tungsha Tao (Pratas Islands). *Acta Oceanogr. Taiwanica* **1995**, *34*, 1–16.
31. Morton, B.; Blackmore, G. South China Sea. *Mar. Pollut. Bull.* **2001**, *42*, 1236–1263. [[CrossRef](#)]
32. McManus, J.W. The Sprately Islands: A marine park? *Ambio* **1994**, *23*, 181–186.
33. Tkachenko, K.S.; Soong, K. Dongsha atoll: A potential thermal refuge for reef-building corals in the South China Sea. *Mar. Environ. Res.* **2017**, *127*, 112–125. [[CrossRef](#)] [[PubMed](#)]
34. Decarlo, T.M.; Cohen, A.L.; Wong, G.T.F. Community production modulates coral reef pH and the sensitivity of ecosystem calcification to ocean acidification. *J. Geophys. Res. Oceans* **2017**, *122*, 745–761. [[CrossRef](#)]
35. Zhao, M.X.; Yu, K.F.; Shi, Q. Coral communities of the remote atoll reefs in the Nansha Islands, southern South China Sea. *Environ. Monit. Assess.* **2013**, *185*, 7381–7382. [[CrossRef](#)] [[PubMed](#)]
36. Zuo, X.; Su, F.; Zhao, H.; Zhang, J.; Wang, Q.; Wu, D. Regional hard coral distribution within geomorphic and reef flat ecological zones determined by satellite imagery of the Xisha Islands, South China Sea. *Chin. J. Oceanol. Limnol.* **2017**, *35*, 501–514. [[CrossRef](#)]
37. Zuo, X.; Su, F.; Zhao, H.; Fang, Y.; Yang, J. Development of a geomorphic classification scheme for coral reefs in the South China Sea based on high-resolution satellite images. *Prog. Geogr.* **2018**, *37*, 1463–1472. (In Chinese)
38. Gong, J.; Zhu, G.; Yang, J.; Zuo, X.; Shi, W. A Study on the object-oriented model for geomorphic unit extraction of coral reefs in the South China Sea. *J. Geo-Inf. Sci.* **2014**, *16*, 997–1004. (In Chinese)
39. Pante, E. *Temporal Variation in a Bahamian Patch Reef Community: The Decline of Rainbow Gardens Reef*; College of Charleston: Charleston, SC, USA, 2005.
40. Veron, J. *Corals of the World*; Australian Institute of Marine Science (AIMS): Townsville, Australia, 2000.
41. Congalton, R.G. Accuracy assessment and validation of remotely sensed and other spatial information. *Int. J. Wildland Fire* **2001**, *10*, 321–328. [[CrossRef](#)]
42. Chun, L.; Jones, B.; Blanchon, P. Lagoon-shelf sediment exchange by storms; Evidence from foraminiferal assemblages, east coast of Grand Cayman, British West Indies. *J. Sediment. Res. A* **1997**, *67*, 17–25.
43. Fujita, K.; Osawa, Y.; Kayanne, H.; Ide, Y.; Yamano, H. Distribution and sediment production of large benthic foraminifers on reef flats of the Majuro Atoll, Marshall Islands. *Coral Reefs* **2009**, *28*, 29–45. [[CrossRef](#)]
44. Taylor, K.E.; Stouffer, R.J.; Meehl, G.A. An overview of CMIP5 and the experiment design. *Bull. Am. Meteorol. Soc.* **2011**, *93*, 485–498. [[CrossRef](#)]
45. Kumar, S.; Merwade, V.; Kinter, J.L.; Niyogi, D. Evaluation of temperature and precipitation trends and long-term persistence in CMIP5 twentieth-century climate simulations. *J. Clim.* **2013**, *26*, 4168–4185.
46. Huang, C.; Qiao, F.; Song, Y.; Li, X. The simulation and forecast of SST in the South China Sea by CMIP5 models. *Acta Oceanol. Sin.* **2014**, *36*, 38–47. (In Chinese)
47. Reynolds, R.W.; Rayner, N.A.; Smith, T.M.; Stokes, D.C.; Wang, W. An improved in situ and satellite SST analysis for climate. *J. Clim.* **1987**, *15*, 1609–1625. [[CrossRef](#)]

48. Hooidonk, R.V.; Huber, M. Effects of modeled tropical sea surface temperature variability on coral reef bleaching predictions. *Coral Reefs* **2012**, *31*, 121–131. [[CrossRef](#)]
49. Church, J.; Clark, P.; Cazenave, A.; Gregory, J.; Jevrejeva, S.; Levermann, A. Sea Level Change. In *Climate Change 2013: The Physical Science Basis*; Intergovernmental Panel on Climate Change, Ed.; Cambridge University: New York, NY, USA, 2013; pp. 1137–1216.
50. Church, J.A.; White, N.J.; Coleman, R.; Lambeck, K.; Mitrovica, J.X. Estimates of the regional distribution of sea level rise over the 1950–2000 period. *J. Clim.* **2004**, *17*, 2609–2625. [[CrossRef](#)]
51. Beckley, B.D.; Zelensky, N.P.; Holmes, S.A.; Lemoine, F.G.; Brown, S.T. Assessment of the Jason-2 extension to the TOPEX/Poseidon, Jason-1 sea-surface height time series for global mean sea level monitoring. *Mar. Geod.* **2010**, *33*, 447–471. [[CrossRef](#)]
52. Yin, J.; Griffies, S.M.; Stouffer, R.J. Spatial variability of sea level rise in twenty-first century projections. *J. Clim.* **2010**, *23*, 4585–4607. [[CrossRef](#)]
53. Yin, J. Century to multi-century sea level rise projections from CMIP5 models. *Geophys. Res. Lett.* **2012**, *39*, L17709. [[CrossRef](#)]
54. Peng, D.; Palanisamy, H.; Cazenave, A.; Meyssignac, B. Interannual sea level variations in the South China Sea Over 1950–2009. *Mar. Geod.* **2013**, *36*, 164–182. [[CrossRef](#)]
55. Leon, J.X.; Woodroffe, C.D. Morphological characterisation of reef types in Torres Strait and an assessment of their carbonate production. *Mar. Geol.* **2013**, *338*, 64–75. [[CrossRef](#)]
56. Perry, C.T.; Kench, P.S.; Murphy, G.N.; Smithers, S.G.; Steneck, R.S.; Mumby, P.J. Estimating rates of biologically driven coral reef framework production and erosion: A new census-based carbonate budget methodology and applications to the reefs of Bonaire. *Coral Reefs* **2012**, *31*, 853–868. [[CrossRef](#)]
57. Hart, D.E.; Kench, P.S. Carbonate production of an emergent reef platform, Warraber Island, Torres Strait, Australia. *Coral Reefs* **2007**, *26*, 53–68. [[CrossRef](#)]
58. Kinsey, D.W.; Hopley, D. The significance of coral reefs as global carbon sinks—Response to greenhouse. *Palaeogeogr. Palaeoclimatol. Palaeoecol.* **1991**, *89*, 363–377. [[CrossRef](#)]
59. Kinsey, D.W.; Davies, P.J. Coral reef growth—A model based on morphological and metabolic studies. *Aust. J. Mar. Sci.* **1975**, *7*, 397–403.
60. Grossman, E.E.; Fletcher, C.H. Holocene reef development where wave energy reduces accommodation space, Kailua Bay, Windward Oahu, Hawaii, U.S.A. *J. Sediment. Res.* **2004**, *74*, 49–63. [[CrossRef](#)]
61. Edinger, E.N.; Limmon, G.V.; Jompa, J.; Widjatmoko, W.; Heikoop, J.M.; Risk, M.J. Normal coral growth rates on dying reefs: Are coral growth rates good indicators of reef health? *Mar. Pollut. Bull.* **2000**, *40*, 404–425. [[CrossRef](#)]
62. Li, S.; Yu, K.F.; Chen, T.R.; Shi, Q.; Zhang, H.L. Assessment of coral bleaching using symbiotic zooxanthellae density and satellite remote sensing data in the Nansha Islands, South China Sea. *Chin. Sci. Bull.* **2011**, *56*, 1031–1037. [[CrossRef](#)]
63. Saunders, M.I.; Albert, S.; Roelfsema, C.M.; Leon, J.X.; Woodroffe, C.D.; Phinn, S.R.; Mumby, P.J. Tectonic subsidence provides insight into possible coral reef futures under rapid sea-level rise. *Coral Reefs* **2016**, *35*, 155–167. [[CrossRef](#)]
64. Van Woesik, R.; Golbuu, Y.; Roff, G. Keep up or drown: Adjustment of western Pacific coral reefs to sea-level rise in the 21st century. *R. Soc. Open Sci.* **2015**, *2*, 150181. [[CrossRef](#)]
65. Davies, P.J.; Montaggioni, L.F. Reef Growth and Sea-level Change: The Environmental Signature. In *Proceedings of the 5th International Coral Reef Congress, Tahiti, French Polynesia, 27 May–1 June 1985*; pp. 477–515.
66. Bridge, T.C.; Hoey, A.S.; Campbell, S.J.; Muttaqin, E.; Rudi, E.; Fadli, N.; Baird, A.H. Depth-dependent mortality of reef corals following a severe bleaching event: Implications for thermal refuges and population recovery. *F1000Research* **2013**, *2*, 187. [[CrossRef](#)]
67. Sheppard, C.R.C. Coral decline and weather patterns over 20 year in the Chagos archipelago, central Indian Ocean. *Ambio* **1999**, *28*, 472–478.
68. Shen, J.; Yang, H.; Wang, Y.; Fu, F.; Zhao, N. Coral community dynamics and shallow-water carbonate deposition of the reef-flat around Yongxing Island, the Xisha Islands. *Sci. China Earth Sci.* **2013**, *56*, 1471–1486. [[CrossRef](#)]
69. Mclean, R.; Kench, P. Destruction or persistence of coral atoll islands in the face of 20th and 21st century sea-level rise. *Wiley Interdiscip. Rev. Clim. Chang.* **2015**, *6*, 445–463. [[CrossRef](#)]
70. Siegle, E.; Costa, M.B. Nearshore wave power increase on reef-shaped coasts due to sea-level rise. *Earths. Future* **2017**, *5*, 1054–1065. [[CrossRef](#)]
71. Shi, X.; Yu, K.F.; Chen, T. Progress in researches on sea-level changes in South China Sea Since mid-Holocene. *Mar. Geol. Quat. Geol.* **2007**, *27*, 121–132.
72. Zhao, J.X.; Yu, K.F. Millennial-, century- and decadal-scale oscillations of Holocene sea-level recorded in a coral reef in the northern South China Sea. In *XVII Inqua Congress*; Pergamon Press: New York, NY, USA, 2007; pp. 167–168.
73. Yu, K. Coral reefs in the South China Sea: Their response to and records on past environmental changes. *Sci. China Earth Sci.* **2012**, *55*, 1217–1229. [[CrossRef](#)]
74. Brown, B.E. Coral Reefs of the Andaman Sea—An Integrated Perspective. In *Oceanography and Marine Biology*; Gibson, R.N., Atkinson, R.J.A., Gordon, J.D.M., Eds.; CRC Press: Boca Raton, FL, USA, 2007; Volume 45, pp. 173–194.
75. Guest, J.R.; Baird, A.H.; Maynard, J.A.; Muttaqin, E.; Edwards, A.J.; Campbell, S.J.; Yewdall, K.; Affendi, Y.A.; Chou, L.M.; Matz, M.V. Contrasting patterns of coral bleaching susceptibility in 2010 suggest an adaptive response to thermal stress. *PLoS ONE* **2012**, *7*, e33353. [[CrossRef](#)]

76. Bento, R.; Hoey, A.S.; Bauman, A.G.; Feary, D.A.; Burt, J.A. The implications of recurrent disturbances within the world's hottest coral reef. *Mar. Pollut. Bull.* **2016**, *105*, 466–472. [[CrossRef](#)]
77. Wall, M. Large-amplitude internal waves benefit corals during thermal stress. *Proc. R. Soc. B* **2014**, *282*, 20140650. [[CrossRef](#)] [[PubMed](#)]
78. Schmidt, G.M.; Wall, M.; Taylor, M.; Jantzen, C.; Richter, C. Large-amplitude internal waves sustain coral health during thermal stress. *Coral Reefs* **2016**, *35*, 869–881. [[CrossRef](#)]
79. Kayanne, H.; Harii, S.; Ide, Y.; Akimoto, F. Recovery of coral populations after the 1998 bleaching on Shiraho Reef, in the southern Ryukus, NW Pacific. *Mar. Ecol. Prog. Ser.* **2002**, *239*, 93–103. [[CrossRef](#)]
80. van Woesik, R.; Sakai, K.; Ganase, A.; Loya, Y. Revisiting the winners and losers a decade after coral bleaching. *Mar. Ecol. Prog. Ser.* **2011**, *434*, 67–76. [[CrossRef](#)]
81. Brown, B.E.; Dunne, R.P.; Somerfield, P.J.; Edwards, A.J.; Naeije, M.C. Long-term impacts of rising sea temperature and sea level on shallow water coral communities over a ~40 year period. *Sci. Rep.* **2019**, *9*, 8826. [[CrossRef](#)]
82. Perry, C.T.; Morgan, K.M. Bleaching drives collapse in reef carbonate budgets and reef growth potential on southern Maldives reefs. *Sci. Rep.* **2017**, *7*, 40581. [[CrossRef](#)]